Vacuum ultraviolet spectra and crystal field analysis of $YAlO_3$ doped with Nd^{3+} and Er^{3+}

Chang-kui Duan and Peter A. Tanner
Department of Biology and Chemistry, City University of Hong Kong, Kowloon, Hong Kong Special Administrative Region, People's Republic of China

Vladimir N. Makhov
Lebedev Physical Institute, Leninskii Prospect 53, 119991 Moscow, Russia and Institute of Physics, University of Tartu, Riia 142, 51014 Tartu, Estonia

Marco Kirm
Institute of Physics, University of Tartu, Riia 142, 51014 Tartu, Estonia

(Received 19 January 2007; revised manuscript received 20 March 2007; published 25 May 2007)

The synchrotron radiation excited emission and excitation spectra are reported at temperatures of 298 and 10 K for $YAlO_3$ (YAP) doped with 1 at. % Nd^{3+} or Er^{3+}. For both systems, no d-f emission is observed and these results are rationalized and compared with other hosts. For YAP:Nd^{3+}, excitation into the $4f^25d$ electronic configuration of Nd^{3+} gives intraconfigurational luminescence from $^2G(2)_{9/2}$ and $^4F_{3/2}$ and there is no evidence for emission from other multiplet terms. Luminescence from $^2P_{3/2}$ is observed for YAP:Er^{3+}, with additional transitions from $^4S_{3/2}$, $^4F_{9/2}$, $^4I_{9/2}$, and $^4I_{11/2}$. The emission spectra have been assigned in detail. The literature energy level datasets are mostly consistent with the derived energy levels from the present study. The f-d excitation spectra show that the lowest d-electron levels are energetically situated below the intrinsic absorption of the host. Crystal field analyses have been performed by using 100 energy levels for each system and the resulting standard deviations were 12.4 and 15.5 cm^{-1} for Er^{3+} and Nd^{3+}, respectively. The multiplet term barycenters are better fitted for the case of Nd^{3+}, whereas crystal field splittings are better modeled for Er^{3+}. The fitted free ion parameters exhibit considerably less uncertainty for Nd^{3+}.

DOI: 10.1103/PhysRevB.75.195130 PACS number(s): 78.55.−m, 32.30.Jc, 71.70.Ch, 32.50.+d

I. INTRODUCTION

The $YAlO_3$ (YAP) crystal is a widely used host for lasers, scintillators, and optical recording media and it comprises the substrate material for thin films of high-temperature superconductors. The YAP crystal crystallizes in the orthorhombically distorted perovskite structure, belonging to the D_{2h}^{16} (*Pnma* or No. 62) symmetry space group, and details can be found in Refs. 1 and 2. Lanthanide ions replace Y^{3+} ions with C_s site symmetry and are surrounded by 12 O^{2-} ligands with Y-O distances ranging from 0.2306 to 0.3010 nm. Detailed experimental investigations of absorption and reflection spectra of the pure compound in the energy range 6.5–42 eV have been presented in Refs. 3–5. Luminescence excitation spectra of intrinsic emissions of pure YAP at liquid helium temperature have been also investigated in the vacuum ultraviolet (VUV). According to the literature the band-gap energy of YAP is 8.8 eV, the maximum of the excitonic absorption is at 8.0 eV, and the onset of intrinsic absorption can be located at 7.6–7.7 eV.[6] The energy band structure of YAP has been calculated recently by Bercha *et al.*[7] The infrared and Raman spectra of $YAlO_3$ (Ref. 8) and $NdAlO_3$ (Ref. 9) have been reported.

The $4f$-$4f$ intraconfigurational spectra of Nd^{3+} and Er^{3+} in $YAlO_3$ have received considerable attention. The detailed scheme of the energy levels of these ions in $YAlO_3$ is depicted in Fig. 1. Antonov *et al.*[10] deduced the complete set of levels for Er^{3+} up to $^4G_{11/2}$ ($\sim$26 500 cm^{-1}) from the 77 K optical spectra. Donlan and Santiago[11] subsequently extended these studies and deduced 104 energy levels from emission and absorption spectra at 4.2 K. The energy levels have been tabulated by Kaminskii[12] and Morrison and Leavitt.[13] The major interest in $YAlO_3$:Er^{3+} has resulted from its laser action. At room temperature, laser action has been observed at 550,[14,15] 851, [16]1.66 μm (Refs. 17–19) (from $^4S_{3/2}$), and 2.7–2.9 μm (Refs. 20–22) (from $^4I_{11/2}$). The population dynamics and decay properties relevant to these laser levels have been investigated.[23,24] The luminescence from the higher multiplet term $^2P_{3/2}$ is concentration quenched.[25] Indeed, such cross-relaxation processes are ubiquitous for Er^{3+} in $YAlO_3$ and are effective in upconversion[26,27] in addition to excited state absorption[28] and photon avalanche[29] processes. Pumping at 1500 nm can provide green and red emission bands.[30] In fact, the first upconversion laser emission reported was from $YAlO_3$:Er^{3+}, which was produced by pumping between 785 and 840 nm giving emission at 550 nm.[31,32] The infrared and red upconversions are a continuing focus of research.[33,34] It is clear that previous emphasis in experimental investigations has been placed upon the structure of lower energy levels of $YAlO_3$:Er^{3+}.

The optical spectra and intensities of Nd^{3+} in $YAlO_3$ have been reported by Weber and Varitimos[35] and the energy levels up to $^2P_{1/2}$ at 23 151 cm^{-1} were assigned from studies at 300 and 85 K. The lowest $^4G_{5/2}$ level was assigned at 16 849 cm^{-1} but apparently this absorption band corresponds to a hot transition from the first Stark level of $^4I_{9/2}$ since it disappears at 4.2 K.[36] Some luminescence transitions of $YAlO_3$:Nd^{3+} have also been investigated by Basiev *et al.*[37] and by Rasuleva and Solomonov.[38] The luminescence from higher energy levels of Nd^{3+} in $YAlO_3$was studied by pump-

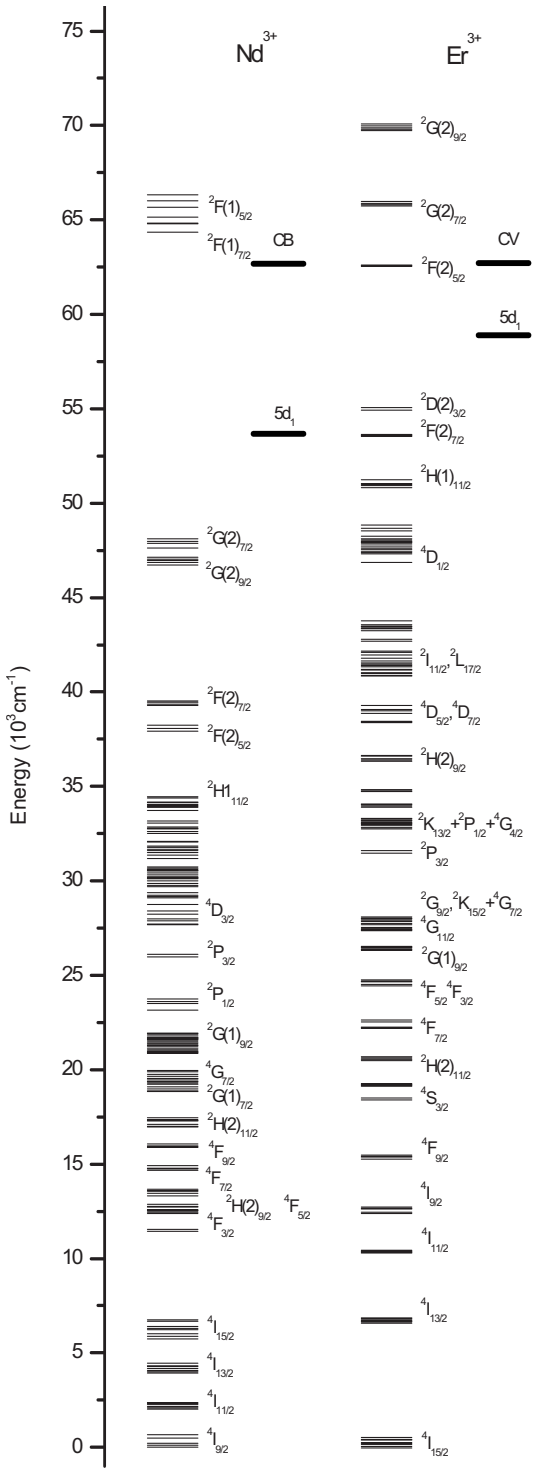

FIG. 1. SLJ energy level schemes of Nd^{3+} and Er^{3+} in YAP from the present energy level calculations. The positions of the measured first peak of the $5d$ level ($5d_1$) and of the host conduction band (CB) are also shown.

ing with intense 808 nm diode radiation so that up to four-photon upconversion was achieved.[39] The Nd^{3+} $4f^25d$ levels were probed by excited state absorption from $^4F_{3/2}$.[40] Laser action has been reported at several wavelengths near 1.1 μm for $YAlO_3:Nd^{3+}$.[41]

Several previous studies have comprised crystal field analyses upon energy level datasets of ions doped into $YAlO_3$ and Karayianis *et al.* were the first to present crystal field parameters for the series.[42] Subsequently, Deb presented multiplet-multiplet line strengths for some luminescence transitions of Er^{3+} and Nd^{3+} in this host[43] and Rukmini *et al.*[44] compared the free-ion parameters from the fitting of multiplet barycenters with those for lanthanide ions in other host lattices. Rukmini *et al.* also performed a correlation crystal field fit of the $YAlO_3:Nd^{3+}$ dataset.[45]

The present work extends the previous spectral investigations of the Nd^{3+} and Er^{3+} ions doped into $YAlO_3$ into the VUV. The synchrotron radiation excited emission and excitation spectra are presented and interpreted. Then, detailed crystal field calculations are carried out for the resulting energy level datasets of the two systems.

II. EXPERIMENTAL DETAILS

The crystals of $YAlO_3$ with nominal dopant ion concentration of Nd^{3+} or Er^{3+} of 1 at. % were kindly donated by Krupa. Emission (200–1000 nm) and excitation (50–300 nm) spectra were measured at the SUPERLUMI station[46] of HASYLAB at DESY (Hamburg) using synchrotron radiation from the DORIS storage ring. Emission spectra were recorded with a 0.3 m Czerny–Turner–type imaging monochromator-spectrograph SpectraPro-308i (Acton Research Corporation) equipped with a liquid nitrogen cooled CCD detector (Princeton Instruments, Inc.). The spectral resolution of the analyzing monochromator with the 300 lines mm^{-1} grating was set to ~0.5 nm. Excitation spectra were recorded with an instrumental resolution of the primary monochromator ~0.3 nm by using a photomultiplier tube (Hamamatsu R6358P) installed in another arm of the analyzing monochromator. The crystal platelets with thickness ~1 mm were polished and mounted onto a copper sample holder attached to a cold finger of a flow-type liquid helium cryostat (Cryovac GmbH).

III. SPECTRA OF Er^{3+} AND Nd^{3+} IN YAP

A. $4f^N$-$4f^N$ emission spectra of Nd^{3+} and Er^{3+} in YAP

The highest energy gerade zone center phonon in YAP has the energy ~630 cm^{-1}.[8] We anticipated that suitably populated $4f^N$ crystal field energy levels would exhibit luminescence in a dilute crystal if the gap below can be spanned by more than four quanta of this vibration (i.e., >2500 cm^{-1}). From the energy level calculations for $YAP:Nd^{3+}$, we therefore located the lowest crystal field levels of $^2F(1)_{7/2}$ (calculated at 64 338 cm^{-1}), $^2G(2)_{9/2}$ (46 718 cm^{-1}), $^2F(2)_{5/2}$ (37 939 cm^{-1}), and $^4F_{3/2}$ (11 421 cm^{-1}) as the sole qualifying candidates below 65 000 cm^{-1}. Furthermore, the first of these energies is above the intrinsic absorption edge of YAP so that luminescence from this level cannot be observable. However, luminescence from other multiplet terms has been assigned by other authors. Rasuleva and Solomonov[38] have recently assigned emission bands in $YAP:Nd^{3+}$ to originate from $^2P_{3/2}$, $^4G_{11/2}$, $^4G_{9/2}$, $^4G_{7/2}$, and $^2D_{5/2}$ but the spectra were not shown. The energy gaps below most of these levels

are $<130\ cm^{-1}$ and therefore, no luminescence can be expected. Basiev *et al.*[37] assigned 77 K luminescence from $^4G_{7/2}$, $^4D_{3/2}$, and $^2P_{3/2}$. The $^2P_{3/2}$ levels were assigned at 25 981 and 26 123 cm^{-1} but our analysis of their figure displaying the $^2P_{3/2}\rightarrow{}^4I_{11/2}$ spectrum places the luminescent states at 25 857 and 25 972 cm^{-1}. The energy gap below $^2P_{3/2}$ was stated as 2222 cm^{-1}. The other two luminescent levels $^4G_{7/2}$ and $^4D_{3/2}$ were assigned from the $^4G_{7/2}\rightarrow{}^4I_{11/2}$ and $^4D_{3/2}\rightarrow{}^4F_{3/2}$ transitions, and the gaps below these levels were stated as 1390 and 1545 cm^{-1}, respectively. These gaps can be spanned by three phonons in $YAlO_3$. These authors also reported luminescence from $^2F(2)_{5/2}$, with crystal field levels at 37 780, 37 890, and 37 967 cm^{-1}. Also the transitions designated to originate from $^4D_{3/2}$ in YAP:Nd^{3+} (Ref. 39, Fig. 8) can be assigned to those purely from $^2P_{3/2}$. Weber has discussed the unlikeliness of emission from $^4D_{3/2}$.[47]

Figure 2 shows the emission spectra at room temperature (a) and at 10 K (b), (c) of YAP:Nd^{3+} excited at energies well below the host intrinsic absorption. All of the emission bands can be assigned to emission from the lowest crystal field levels of $^2G(2)_{9/2}$ (with the lowest energy level inferred to be at 46 718 cm^{-1}) and $^4F_{3/2}$ (located at 11 425 cm^{-1}), which both have significant spacings to the next lower levels. The terminal multiplet terms are marked in Fig. 2(b), and the crystal field energy levels of the ground multiplet are marked in Fig. 2(c). It is interesting that the luminescence transitions from $^2G(2)_{9/2}$ which terminate upon ^4I_J ($2J=9$, 11, 13, 15) are very weak, as essentially found for Nd^{3+} in YAG. The derived energy levels are compared with those from previous studies and from calculations in Table I. Some transitions are barely distinguished from the noise levels in the spectrum of Fig. 2(b) and are listed in parentheses. In addition to the poor resolution, there is error in determining the terminal crystal field levels because two large numbers are being subtracted. For these reasons, the energy level fitting (discussed in Sec. IV C) did not employ additional energy levels derived from the present study except for $^2G(2)_{9/2}$ at 46 718 cm^{-1}. With those considerations taken into account, the agreement of the derived energy levels with previous studies and with the calculations of the present study as displayed in Table I is considered satisfactory. The only multiplet term crystal field levels which are located at rather different energies from calculation are some of the higher energy levels, notably levels 135–137 of $^2L_{17/2}$.

Only one feature in Fig. 2(b) then remains unassigned and corresponds to the starred band at 22 818 cm^{-1}. However, there is no evidence for luminescence from multiplet terms other than from $^2G(2)_{9/2}$ and $^4F_{3/2}$. The transitions from the latter multiplet term to the crystal field levels of the $^4I_{9/2}$ ground state are shown in Fig. 2(c), with their derived energies marked. Comparison with the room temperature spectrum, Fig. 2(a), enables the energies of thermally populated luminescent crystal field levels to be experimentally located at 11 552 cm^{-1} (level No. 28: $^4F_{3/2}$) and 46 899±7 cm^{-1} [No. 168: $^2G(2)_{9/2}$].

Emission spectra of YAP:Er^{3+} (1 at. %) at 300 and 10 K excited by 167 nm radiation are shown in Fig. 3. The highest energy weak emission, near 318 nm, is due to the $^2P_{3/2}\rightarrow{}^4I_{15/2}$ transition. Stronger emission bands, near 403 and

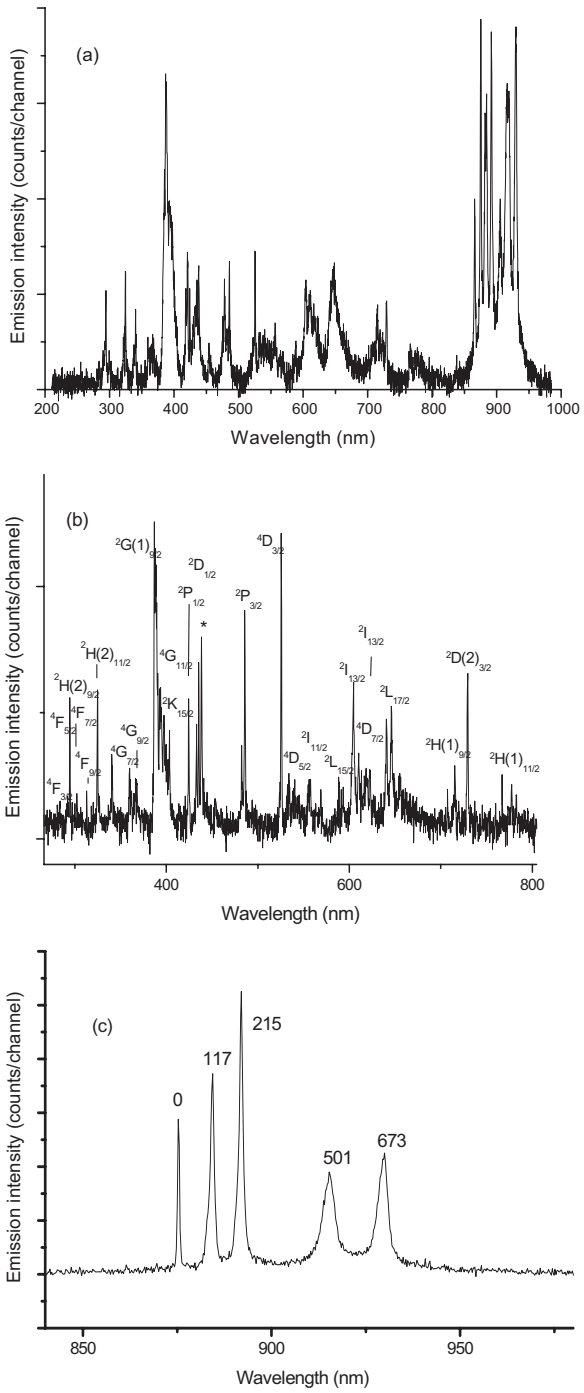

FIG. 2. Emission spectra of $YAlO_3$:Nd^{3+} (1 at. %): (a) recorded at room temperature under excitation by 180 nm photons; (b), (c) at 10 K under excitation by 175 nm photons. The luminescent state is $^2G(2)_{9/2}$ at 46 718 cm^{-1}, with the exception of the lowest energy bands that correspond to the $^4F_{3/2}\rightarrow{}^4I_{9/2}$ transition. The terminal multiplet terms are labeled in (b). The ground state crystal field energy levels are labeled in (c).

475 nm, are due to transitions to the terminal $^4I_{13/2,11/2}$ multiplet terms. Other transitions from $^2P_{3/2}$ are also marked in Fig. 3(b), but it is clear that other luminescent states $^4S_{3/2}$, $^4F_{9/2}$, $^4I_{9/2}$, $^4I_{11/2}$ are also populated due to nonradiative decay processes from $^2P_{3/2}$ including cross-relaxation.[25] The $^2P_{3/2}$ radiative intensity branching ratios to terminal multi-

TABLE I. Comparison of derived energy levels from the $^2G(2)_{9/2}$ luminescence spectrum of YAP:Nd^{3+} with values from the literature and calculations (calc., Sec. IV C). [Level 27 is located at 11 425 cm^{-1} in Fig. 2(c)].

Level	SLJ	Energy (cm^{-1})		
		Literature[a]	Calc.	Derived from Fig. 2(b)
27	$^4F_{3/2}$	11 421	11 427	11 429
35	$^2H(2)_{9/2}$	12 742	12 774	12 745
41	$^4S_{3/2}$	13 605	13 605	13 607
45	$^4F_{9/2}$	14 740	14 744	14 742
50	$^2H(2)_{11/2}$	15 903	15 915	15 912
58	$^2G(1)_{7/2}$	17 313	17 330	17 330
59	$^2G(1)_{7/2}$	17 364	17 355	
60	$^2G(1)_{7/2}$	17 456	17 458	
61	$^4G_{7/2}$	18 846	18 841	18 846
62	$^4G_{7/2}$	18 893	18 895	18 920
63	$^4G_{7/2}$	18 975	18 983	18 997
64	$^4G_{7/2}$	19 077	19 100	19 090
65	$^2K_{13/2}$	19 245	19 242	19 247
66	$^2K_{13/2}$	19 309	19 304	
67	$^4G_{9/2}$	19 350	19 364	19 361
68	$^4G_{9/2}$		19 396	
69	$^4G_{9/2}$	19 425	19 417	19 424
70	$^4G_{9/2}$		19 501	19 497
71	$^4G_{9/2}$		19 520	
72	$^2K_{13/2}$	19 546	19 556	19 550
77	$^2G(1)_{9/2}+^2D_{3/2}$	20 865	20 862	20 869
78	$^2G(1)_{9/2}+^2D_{3/2}$		20 880	
79	$^2G(1)_{9/2}+^2D_{3/2}$	20 894	20 899	
80	$^2G(1)_{9/2}+^2D_{3/2}$	20 955	20 950	20 939
81	$^2G(1)_{9/2}+^2D_{3/2}$		20 983	20 992
82	$^2G(1)_{9/2}+^2D_{3/2}$	21 041	21 040	21 043
83	$^2G(1)_{9/2}+^2D_{3/2}$	21 110	21 107	21 111
84	$^4G_{11/2}+^2K_{15/2}$	21 231	21 219	
85	$^4G_{11/2}+^2K_{15/2}$	21 276	21 269	21 247
86	$^4G_{11/2}+^2K_{15/2}$	21 294	21 315	21 302
87	$^4G_{11/2}+^2K_{15/2}$	21 367	21 379	21 356
88	$^4G_{11/2}+^2K_{15/2}$	21 464	21 467	(21 488)
89	$^2G_{11/2}+^2K_{15/2}$	21 536	21 513	21 543
90	$^4G_{11/2}+^2K_{15/2}$	21 580	21 578	21 585
91	$^4G_{11/2}+^2K_{15/2}$	21 630	21 628	
92	$^4G_{11/2}+^2K_{15/2}$	21 654	21 646	(21 659)
93	$^4G_{11/2}+^2K_{15/2}$	21 718	21 708	
94	$^4G_{11/2}+^2K_{15/2}$	21 748	21 747	
95	$^4G_{11/2}+^2K_{15/2}$	21 834	21 846	21 831
96	$^4G_{11/2}+^2K_{15/2}$	21 906	21 911	21 923
97	$^4G_{11/2}+^2K_{15/2}$	21 930	21 938	
98	$^2P_{1/2}$	23 164	23 162	23 158
99	$^2D(1)_{5/2}$	23 463	23 500	
100	$^2D(1)_{5/2}$	23 635	23 610	23 623
101	$^2D(1)_{5/2}$	23 759	23 750	23 747
102	$^2P_{3/2}$	25 981	25 982	25 984
103	$^2P_{3/2}$	26 123	26 126	26 130
104	$^4D_{3/2}$	27 668[b]	27 669	
105	$^4D_{3/2}$	27 726[b]	27 725	27 690
106	$^4D_{5/2}$		27 891	
107	$^4D_{5/2}$		27 979	(27 988)
117	$^4D_{7/2}$		29 757	(29 727)
118	$^2L_{15/2}$		29 865	(29 857)
123	$^2L_{15/2}$		30 175	30 175
124	$^2L_{15/2}$		30 223	
125	$^4D_{7/2}$		30 304	30 328
126	$^2L_{15/2}$		30 316	
127	$^2L_{15/2}$		30 429	(30 410)
128	$^2I_{13/2}$		30 518	(30 504)
129	$^2I_{13/2}$		30 553	(30 542)
130	$^2I_{13/2}$		30 585	
131	$^2I_{13/2}$		30 605	
132	$^2I_{13/2}$		30 651	(30 655)
133	$^2I_{13/2}$		30 661	
134	$^2I_{13/2}$		30 751	
135	$^2L_{17/2}$		31 182	31 110
136	$^2L_{17/2}$		31 351	31 237
137	$^2L_{17/2}$		31 515	(31 454)
144	$^2H(1)_{9/2}$		32 515	(32 579)
145	$^2H(1)_{9/2}$		32 613	
146	$^2H(1)_{9/2}$		32 740	32 739
147	$^2H(1)_{9/2}$		32 787	
148	$^2H(1)_{9/2}$		32 848	
149	$^2D(2)_{3/2}$		33 073	33 005
150	$^2D(2)_{3/2}$		33 180	
151	$^2H(1)_{11/2}$		33 714	(33 677)
152	$^2D(2)_{5/2}$		33 910	(33 855)
153	$^2D(2)_{5/2}$		33 921	(33 936)
159	$^2H(1)_{11/2}$		34 448	
160	$^2F(2)_{5/2}$		37 939	
166	$^2F(2)_{7/2}$		39 520	
167	$^2G(2)_{9/2}$		46 718	46 718
168	$^2G(2)_{9/2}$		46 869	
175	$^2G(2)_{7/2}$		48 120	
176	$^2F(1)_{7/2}$		64 338	
182	$^2F(1)_{5/2}$		66 312	

[a]Reference 12.
[b]Reference 37.

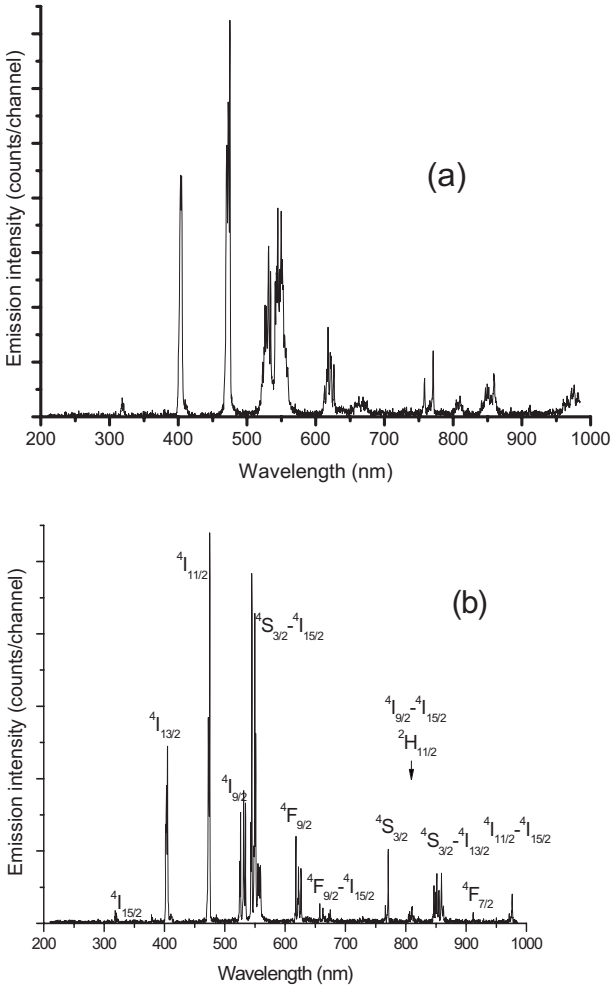

FIG. 3. Emission spectra of $YAlO_3:Er^{3+}$ (1 at. %) at room temperature (a) and 10 K (b) excited by 167 nm photons. In (b) the multiplet-multiplet transitions are fully marked except where the initial multiplet term is $^2P_{3/2}$ and only the terminal term is indicated.

plets are in agreement with the calculations of Kaminskii *et al.*[14] The fine structure in the survey spectrum as presented in Fig. 3(b) is not evident, but a detailed analysis in an enlarged scale provides an energy level dataset which is in agreement with the literature energy levels.[12]

The excitation spectrum of the $^2P_{3/2} \rightarrow {}^4I_{11/2}$ emission at 473 nm was recorded in the range from 300 to 75 nm and is shown in Fig. 4. The sharp peaks of the excitation spectrum in the range 185–285 nm feature the $4f^{11}$-$4f^{11}$ absorptions of Er^{3+}. The strength of these absorptions can be calculated in the frame of Judd-Ofelt theory using the intensity parameters $\Omega_2=1.06$, $\Omega_4=2.63$, $\Omega_6=0.78$ (units, 10^{-20} cm^2) from Ref. 48 and the square modulus of the reduced matrix elements of $U^{(k)}$ ($k=2, 4, 6$) presented by Kaminskii *et al.*[14] These calculations show that those absorption bands from the ground multiplet term are all predominantly contributed by the Ω_4 parameter associated with $U^{(4)}$ and the calculated intensities shown in Fig. 4 are in reasonable agreement with the observed intensities.

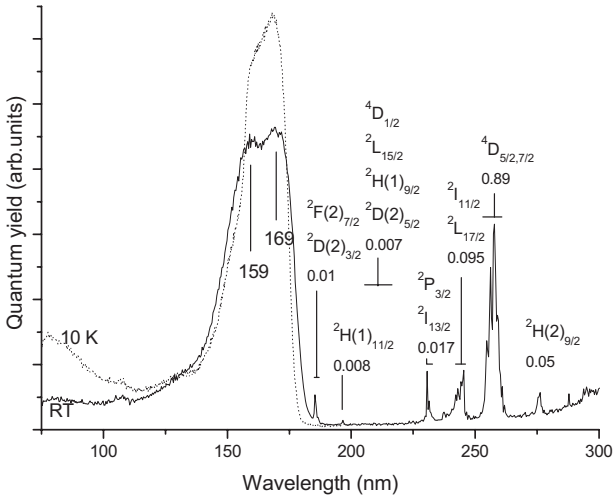

FIG. 4. Excitation spectrum of the 473 nm emission of $YAlO_3:Er^{3+}$ (1 at. %) at 10 K. The initial state is $^4I_{15/2}$ and the terminal $4f^{11}$ multiplet terms are marked together with the calculated intensities from the Ω_4 parameter alone.

B. $4f^N$-$4f^{N-1}5d$ excitation spectra of Nd^{3+} and Er^{3+} in YAP

The higher energy excitation spectrum of YAP:Er^{3+} is also depicted in Fig. 4, whereas Fig. 5 shows the corresponding excitation spectrum of YAP:Nd^{3+}. Both spectra show intense broad bands with onsets at wavelengths shorter than 200 nm. These features exhibit peaks at 186, ~159 nm for Nd^{3+} and at 169, ~159 nm for Er^{3+}. The excitation spectrum of YAP:Ce^{3+} exhibits a peak at 154 nm (Ref. 3) or 163 nm (Ref. 49) which has been attributed to the excitonic absorption of YAP.[3] This is also in good agreement with the onset of self-trapped exciton luminescence excitation as reported by Lushchik *et al.*[6] Therefore the features at ~159 nm in the present study are also associated with the intrinsic excitonic transition. The excitation spectrum of the self-trapped exciton emission from a pure YAP crystal is shown by the circles

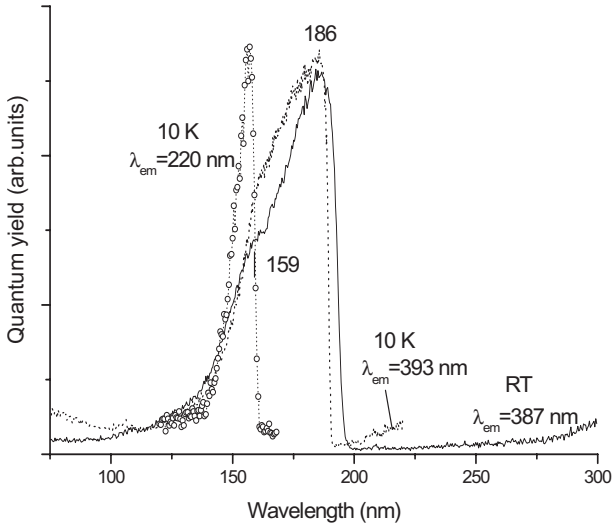

FIG. 5. Excitation spectra of $YAlO_3:Nd^{3+}$ (1 at. %) at room temperature and 10 K. The circled points show the excitation spectrum of self-trapped exciton emission from pure YAP at 10 K.

TABLE II. The first (spin-allowed) f-d absorption peak for lanthanide ions in four hosts.

Host	LaF_3 (Ref. 50)		$LiYF_4$ (Ref. 50)		YPO_4 (Refs. 51 and 52)		$YAlO_3$ (Ref. 50)	
	eV	nm	eV	nm	eV	Nm	eV	nm
Pr^{3+}	6.6	188	5.8	213	5.6	227	5.6	223
Nd^{3+}	7.8	159	7.1	176	6.7	186	6.6	188
Eu^{3+}	9.5	131	8.7	143	8.2	152		
Er^{3+}	8.6	145	8.0	155	7.7	161		

in Fig. 5 and the band maximum corresponds to the maxima at ~159 nm in the excitation spectra of the Nd^{3+} and Er^{3+} emission. Hence, the lower energy intense bands in Figs. 4, and 5 have different origins and may originate from $4f^N$-$4f^{N-1}5d$ transitions of Ln^{3+}. In fact, from excited state absorption experiments, the first peak of $4f^3$-$4f^25d$ transitions in YAP:Nd^{3+} has been reported to be at about 188 nm.[40] To the best of our knowledge, there is no previous report on the f-d absorption spectrum of YAP:Er^{3+}. Based on the data of f-d absorption spectra of several lanthanide ions in various hosts shown in Table II, we estimate that the spin-allowed f-d absorption band of Er^{3+} in YAP would be at 7.4 ± 0.13 eV (59 500 cm^{-1}; 168 nm) by a linear extrapolation. This value is close to that observed in Fig. 4. In YAP, the $5d$ states of Ce^{3+} split into five crystal field energy levels as a result of C_s site symmetry. The splitting of the $5d$ crystal field levels shown in the $4f$-$5d$ absorption of YAP:Ce^{3+} (Ref. 53) is 0, 1400, 3300, 8300, and 12 100 cm^{-1}, with the first three spectral peaks being very strong and the last two very weak. Van Pietersen *et al.*[52] have shown that $5d$ crystal field splittings of Er^{3+} are roughly comparable to those of Ce^{3+} in a variety of host lattices. Thus, assuming the first peak to be at 167 nm for YAP:Er^{3+}, the other four f-d absorption bands would be at ~163, 158, 147, and 139 nm, with the last two very weak. Thus it is clear that most of the higher energy $5d$ bands in YAP:Er^{3+} fall into the region of the stronger host absorption and will not be seen in the excitation spectrum.

Estimation of the first two $5d$ crystal field level splittings in YAP:Nd^{3+} from the figure of the excited state absorption spectrum in Ref. 40 gives the values 1810 and 4100 cm^{-1}, which then infers the respective f-d transitions from the ground state to be at 180 and 173 nm, i.e., well below the host absorption. However, these higher-energy $4f$-$5d$ transitions are not resolved in Fig. 4 because of the complete absorption of exciting radiation by f-d transitions leading to the saturation of spectra.

The energies of the lowest $5d$ states of Er^{3+} and Nd^{3+} are therefore both below the intrinsic absorption edge of YAP. However, $5d$-$4f$ emission was not observed for Er^{3+} or Nd^{3+} in YAP, even using the technique of time-resolved measurements on the nanosecond timescale. Obviously, for Er^{3+}, the excitation of $4f^{10}5d$ levels leads to fast nonradiative relaxation to the lowest $5d$ (high-spin) level, which should be located somewhere below the edge of spin-allowed f-d absorption at ~55 000 cm^{-1}, taking into account the energy difference between high- and low-spin $5d$ levels of Er^{3+}.[50] Then the lowest $5d$ level will relax to some f-electron levels almost resonantly. This explains why $5d$-$4f$ emission is not observed. In the case of YAP:Nd^{3+}, the $5d$ absorption edge is about 52 000 cm^{-1}. The gap between this and the $^2G(2)_{7/2}$ multiplet of $4f^3$ (48 120 cm^{-1}) is <4000 cm^{-1}. However, the much stronger electron-phonon coupling between $5d$ levels and lattice vibrations can permit the nonradiative relaxation from the $5d$ levels to $^2G(2)_{7/2}$ (see, e.g., the configuration coordinate diagram for Nd^{3+} in KYF_4 in Ref. 54), thus explaining why no $5d$-$4f$ emission is observed.

IV. CRYSTAL FIELD ENERGY LEVEL FITTING OF Er^{3+} AND Nd^{3+} IN YAP

A. Crystal field Hamiltonian and parameters for $4f^N$ configuration in YAP

The energy levels of the $4f^N$ configuration of a lanthanide ion in a crystal can be analyzed with the following general crystal field Hamiltonian:

$$H = E_{\text{avg}} + \sum_{k=2,4,6} F^k \hat{f}_k + \zeta_{4f} \sum_{i=1}^{N} \hat{s}_i \cdot \hat{l}_i + \alpha \hat{\mathbf{L}}^2 + \beta \hat{G}(G_2) + \gamma \hat{G}(R_2) + \sum_{j=0,2,4} M^j \hat{m}_j + \sum_{k=2,4,6} P^k \hat{p}_k + \sum_{r=2,3,4,6,7,8} T^r \hat{t}_r + \sum_{k=2,4,6} \sum_{q=-k}^{k} B_q^k C_q^{(k)}. \quad (1)$$

Here all the interaction operators and the parameters for their strength are written in the usual practice (see, for example, Ref. 55), with 20 adjustable "atomic" parameters. Lanthanide ions doped in YAP generally substitute at the Y site of C_s symmetry, where the allowed (nonzero) crystal field parameters are limited to k, q even. This, together with the restriction of $B^k_{-q}=(-1)^q(B^k_q)^*$ (where the asterisk means complex conjugate) imposed by the hermiticity of the Hamiltonian, limits the number of independent real parameters to be 15, i.e., including three real crystal field parameters B^k_0 $(k=2,4,6)$ and the six complex B^k_q $[(k,q)=(2,2),(4,2),(4,4),(6,2),(6,4),(6,6)]$ which each require two parameters. A given set of all the 15 real parameters for crystal field interaction and 20 real "atomic" parameters (including 1 for E_{avg}) for quasi-free-ion interaction completely specify the Hamiltonian given as a matrix under a routine choice of bases for a given $4f^N$ configuration, and the diagonalization produces all the eigenvalues of the $4f^N$ states. Since only the z axis can be solely specified for C_s site symmetry, then a suitable rotation in the x-y plane can transform one complex B^k_q parameter to be real without changing the

eigenvalues. Thus the number of independent real parameters for crystal field interaction is reduced to 14. The atomic parameters were further constrained in the fittings as described below.

There is still the lack of an accurate *ab initio* method to calculate the $4f^N$ energy levels of lanthanide ions in crystals down to the level of $\sim 100\ \mathrm{cm}^{-1}$ for comparison with the measured values, so that the general practice is to assign the parameters in the Hamiltonian with reasonable estimated initial values and then to optimize iteratively by minimizing the following quantity:

$$\delta^2 = \sum_{i=1}^{N_{\mathrm{cf}}} (E_i^{\mathrm{exp}} - E_i^{\mathrm{calc}})^2 \tag{2}$$

where N_{cf} is the number of measured crystal field energy levels. It is well known that the value of δ^2 depends on the number of parameters freely adjustable in the optimization. The free ion parameters mostly adjust the center of gravity of each multiplet whereas the crystal field parameters mostly govern the splitting of energy levels from the center of gravity of the corresponding multiplet. We denote the number of multiplets that the N_{cf} energy levels cover by N_{cg}; the multiplet that the ith energy level belongs to by $j(i)$; the number of measured energy levels for multiplet j $(j=1,\ldots,N_{\mathrm{cg}})$ by g_j; and the difference between the measured and calculated center of gravity for multiplet j as ΔE_j^{fi}. Then the δ^2 defined in Eq. (2) can be written by introducing σ_{tot}, σ_{cf}, and σ_{fi}, as

$$\sigma_{\mathrm{tot}} = \sqrt{\frac{\delta^2}{N_{\mathrm{cf}} - N_{\mathrm{cfp}} - N_{\mathrm{fip}}}}, \tag{3}$$

$$\sigma_{\mathrm{cf}} = \sqrt{\frac{\sum_{j=1}^{N_{\mathrm{cf}}} (E_i^{\mathrm{exp}} - E_i^{\mathrm{calc}} - \Delta E_{j(i)}^{\mathrm{fi}})^2}{N_{\mathrm{cf}} - N_{\mathrm{cg}} - N_{\mathrm{cfp}}}}, \tag{4}$$

$$\sigma_{\mathrm{fi}} = \sqrt{\frac{\sum_{j=1}^{N_{\mathrm{cg}}} g_j (\Delta E_j^{\mathrm{fi}})^2}{N_{\mathrm{cg}} - N_{\mathrm{fip}}}}, \tag{5}$$

$$\delta^2 = (N_{\mathrm{cf}} - N_{\mathrm{cfp}} - N_{\mathrm{fip}})\sigma_{\mathrm{tot}}^2 \tag{6}$$

$$= \sum_{i=1}^{N_{\mathrm{cf}}} (E_i^{\mathrm{exp}} - E_i^{\mathrm{calc}} - \Delta E_{j(i)}^{\mathrm{fi}})^2 + \sum_{j=1}^{N_{\mathrm{cg}}} g_i (\Delta E_j^{\mathrm{fi}})^2 \tag{7}$$

$$= (N_{\mathrm{cf}} - N_{\mathrm{cg}} - N_{\mathrm{cfp}})\sigma_{\mathrm{cf}}^2 + (N_{\mathrm{cg}} - N_{\mathrm{fip}})\sigma_{\mathrm{fi}}^2. \tag{8}$$

Here σ_{tot}, σ_{cf}, and σ_{fi} reflect the total residual error, the residual error related to crystal field splitting, and that related to center of gravity of multiplets, respectively. N_{cfp} and N_{fip} are the number of crystal field and free ion parameters, respectively. In general, the optimization of free ion parameters mostly reduces σ_{fi}, with weak impact on σ_{cf} through the wave functions of multiplets; whereas optimization of crystal field parameters mainly reduces σ_{cf}, with weak impact on σ_{fi} due to multiplet mixing and incompletely measured energy levels for a multiplet.

B. Theoretical results for YAP:Er^{3+}

In this optimization the initial values of free ion parameters were taken from those of Er^{3+} in LaF_3 and then these were refined by a least squares optimization of calculated quasi-free-ion energy levels against the barycenter of the measured crystal field energy levels for each multiplet. Then the free ion parameters were used together with values of crystal field parameters taken from Ref. 43 to produce a list of calculated energy levels which was used to assign the measured crystal field energy levels. The assignment was done by two steps. In the first step, all the energy levels presented in Refs. 11 and 13 were employed, except those suspect ones with weak intensity and linewidth of more than $10\ \mathrm{cm}^{-1}$, and those which cannot be uniquely assigned. Then the optimization of parameters was done to produce calculated energy levels for the second step of assignment, where those experimental energy levels left over from the first step were assigned to calculated energy levels wherever possible. The calculation was performed for the full basis space spanned by $4f^{11}$ with corrected three-body matrix elements for $4f^{11}$ instead of those for $4f^3$ used previously in many historical calculations. This has some apparent effects on the optimized values of free ion parameters. The missed few lines in the data file for the matrix elements of $\hat{m}_j$ $(j=0,2,4)$ and $\hat{p}_k$ $(k=2,4,6)$ in many of the previous calculations are included in our calculations. The optimization was done first for free-ion parameters and then for crystal field parameters and then all parameters were allowed to vary, except those without well-defined values (i.e., those in Table III enclosed by square brackets), which were fixed in the last step of optimization. The final parameters and other related quantities for Er^{3+} are given in the left part of Table III. To check the sensitivity to the initial values, we have also performed the fitting using the values provided by O'Hare and Donlan.[56] A set of parameter values within the uncertainties given in Table III was obtained. Note that the imaginary part of B_4^6 was constrained to zero because of its great uncertainty. Thus, altogether 15 free ion parameters and 13 crystal field parameters were employed in the fitting as variable parameters. The calculated energies of all crystal field levels of the $4f^{11}$ configuration are listed in Table IV together with the corresponding 100 measured energy levels.

Some detailed comments are provided here. It is noted that the suspected broad peaks located at 27 683, 27 775, 28 044, 28 077, and 33 375 cm^{-1} do not fit with the calculated energy levels and were not included in the optimization. The measured level 22 636 cm^{-1} is taken from Ref. 10 and is corrected for the temperature shift. The first four of the excluded peaks are very near to the calculated energy levels 27 663, 27 764, 28 084 cm^{-1}, which correspond to the measured levels at 26 670, 27 760, and 28 065 cm^{-1}. The calculated energy of the level nearest to the very weak and broad

TABLE III. The results of the least square optimizations for YAP:Ln^{3+}. All parameter values are in cm^{-1}. Constrained values are in square brackets.

System	YAP:Er^{3+}		YAP:Nd^{3+}	
Parameter	Value	Uncertainty	Value	Uncertainty
E_{avg}	35 526.6	±12.7	24 119	±3
F^2	95 598.4	±154.5	70 925	±25
F^4	65 423.0	±512.6	50 794	±67
F^6	51 615.9	±553.8	35 424	±63
α	17.5	±0.4	23	±0.2
β	−637.0	±12.4	−691	±8
γ	2568.2	±172.8	[1690]	
M^0	4.46	±0.26	1.9	±0.2
M^2	$[0.56\,M^0]$		$[0.56\,M^0]$	
M^4	$[0.38M^0]$		$[0.38M^0]$	
P^2	776.6	±74.1	206	±39
P^4	$[0.75\,P^2]$		$[0.75\,P^2]$	
P^6	$[0.5\,P^2]$		$[0.5\,P^2]$	
T^2	[400.0]		458	±9
T^3	44.8	±3.4	38.4	±3.4
T^4	62.5	±5.1	75.8	±5.3
T^6	−324.7	±13.3	−290	±10
T^7	337.4	±27.2	237	±11
T^8	435.7	±38	496	±28
ζ_{4f}	2373.4	±1.9	875	±2
B_0^2	−178.5	±33.4	−154	±47.90
B_2^2	489.6	±15.1	578	±18
B_0^4	−134.0	±71.6	−541	±79
B_2^4	$464-183i$	$\pm(53+74i)$	$967+24i$	$\pm(39+74i)$
B_4^4	$-9+627i$	$\pm(55+45i)$	$-309+608i$	$\pm(62+62i)$
B_0^6	−453	±101	−671	±97
B_2^6	$199-62i$	$\pm(69+67i)$	$(512-18i)$	$\pm(65+145i)$
B_4^6	$808+[0i]$	±42	$1611+[0i]$	±35
B_6^6	$-74+24i$	$\pm(58+60i)$	$0+132i$	$\pm(52+107i)$
N_{cf}	100		100	
N_{fip}	15		15	
N_{cfp}	13		13	
N_{cg}	21		18	
σ_{cf}	10.8		15.6	
σ_{fi}	24.0		13.5	
σ_{tot}	12.4		15.5	

TABLE IV. The measured (Ref. 11) and calculated (using the parameters given in Table III) energy levels for YAP:Er^{3+}. All energies are in cm^{-1}.

Multiplet	$E_{freeion}$	Level	Ref. 11	Calc.	Difference
$^4I_{15/2}$	262	1	0	−9	9
		2	51	48	3
		3	171	164	7
		4	218	212	6
		5	266	268	−2
		6	388	387	1
		7	443	435	8
		8	516	530	−14
$^4I_{13/2}$	6727	9	6602	6589	13
		10	6641	6635	6
		11	6669	6667	2
		12	6715	6712	3
		13	6773	6761	12
		14	6814	6807	7
		15	6868	6866	2
$^4I_{11/2}$	10 355	16	10 282	10 283	−1
		17	10 293	10 303	−10
		18	10 322	10 337	−15
		19	10 347	10 359	−12
		20	10 382	10 395	−13
		21	10 402	10 426	−24
$^4I_{9/2}$	12 574	22	12 393	12 389	4
		23	12 446	12 446	0
		24	12 624	12 618	6
		25	12 648	12 650	−2
		26	12 732	12 742	−10
$^4F_{9/2}$	15 378	27	15 263	15 269	−6
		28	15 344	15 357	−13
		29	15 374	15 377	−3
		30	15 396	15 400	−4
		31	15 481	15 486	−5
$^4S_{3/2}$	18 462	32	18 406	18 405	1
		33	18 487	18 488	−1
$^2H(2)_{11/2}$	19 219	34	19 119	19 120	−1
		35	19 162	19 177	−15
		36	19 190	19 189	1
		37	19 240	19 227	13
		38	19 275	19 263	12
		39	19 303	19 282	21
$^4F_{7/2}$	20 579	40	20 482	20 472	10
		41	20 555	20 548	7
		42	20 617	20 618	−1
		43	20 685	20 686	−1

TABLE IV. (*Continued.*)

Multiplet	E_{freeion}	Level	Ref. 11	Calc.	Difference
$^4F_{5/2}$	22 237	44	22 196	22 200	−4
		45	22 227	22 225	2
		46	22 259	22 263	−4
$^4F_{3/2}$	24 537	47	22 526	22 526	0
		48	22 636	22 635	1
$^2G(1)_{9/2}$	24 632	49	24 479	24 461	18
		50	24 526	24 521	5
		51	24 666	24 652	14
		52	24 698	24 684	14
		53	24 766	24 761	5
$^4G_{11/2}$	26 438	54	26 308	26 328	−20
		55	26 322	26 352	−30
		56	26 381	26 396	−15
		57	26 459	26 453	6
		58	26 476	26 487	−11
		59	26 526	26 518	8
$^4G_{9/2}$	27 398	60	27 352	27 354	−2
		61	27 381	27 369	12
		62	27 399	27 389	10
		63	27 411	27 408	3
		64	27 445	27 437	8
$^2K_{15/2}$+	27 751	65	27 487	27 482	5
$^4G_{7/2}$	27 975	66	27 544	27 543	1
		67	27 670	27 667	3
		68	27 732	27 733	−1
		69	27 761	27 762	−1
		70		27 856	
		71	27 913	27 931	−18
		72		27 972	
		73		27 987	
		74	27 997	28 007	−10
		75		28 013	
		76	28 065	28 080	−15
$^2P_{3/2}$	31 540	77	31 449	31 448	1
		78	31 585	31 591	−6
$^2K_{13/2}$+	33 010	79	32 773	32 763	10
$^2P_{1/2}$+	33 075	80	32 823	32 818	5
$^4G_{5/2}$	33 194	81		32 915	
		82	32 983	32 984	−1
		83		33 019	
		84	33 061	33 051	10
		85		33 115	
		86	33 162	33 175	−13
		87	33 219	33 213	6
		88	33 302	33 288	14
		89		33 319	

TABLE IV. (*Continued.*)

Multiplet	E_{freeion}	Level	Ref. 11	Calc.	Difference
$^4G_{7/2}$	33 973	90	33 866	33 899	−33
		91	33 962	33 961	2
		92	34 038	34 028	10
		93	34 089	34 068	21
$^2D(1)_{5/2}$	34 791	94	34 739	34 732	7
		95	34 775	34 781	−6
		96	34 827	34 829	−2
$^2H(2)_{9/2}$	36 493	97	36 315	36 324	−9
		98	36 389	36 406	−17
		99	36 463	36 464	−1
		100		36 621	
		101	36 663	36 646	17
$^4D_{5/2}$	38 430	102		38 398	
		103	38 425	38 415	10
		104		38 458	
$^4D_{7/2}$	39 042	106		38 998	
		107	39 076	39 085	−9
		108	39 312	39 293	19
$^2I_{11/2}$	40 988	109		40 848	
		114		41 146	
$^2L_{17/2}$	41 511	115		41 164	
		123		41 976	
$^4D_{3/2}$	42 135	124		42 108	
		125		42 177	
$^2D_{3/2}$	42 741	126		42 692	
		127		42 782	
$^2I_{13/2}$	43 447	128		43 253	
		134		43 760	
$^4D_{1/2}$	46 862	135		46 867	
$^2L_{15/2}$	47 675	136		47 309	
$^2D(2)_{5/2}$	48 665	151		48 833	
$^2H(1)_{11/2}$	50 996	152		50 815	
		157		51 257	
$^2F(2)_{7/2}$	53 574	158		53 524	
		161		53 646	
$^2D(2)_{3/2}$	55 001	162		54 937	
		163		55 081	
$^2F(2)_{5/2}$	62 577	164		62 551	
		166		62 608	
$^4G(2)_{7/2}$	65 846	167		65 743	
		170		65 978	

TABLE IV. (*Continued.*)

Multiplet	E_{freeion}	Level	Ref. 11	Calc.	Difference
$^2G(2)_{9/2}$	69 893	171		69 742	
		175		70 095	
$^2F(1)_{5/2}$	90 930	176		90 662	
		178		91 255	
$^2F(1)_{7/2}$	95 888	179		95 534	
		182		96 347	

measured peak at 33 375 cm^{-1} is 33 316 cm^{-1}. This and another weak and broad peak 33 219 cm^{-1} that has a corresponding calculated energy level 33 213 cm^{-1} were only included in the last step of the optimization.

The fitting of 100 levels by letting 15 free ion parameters (N_{fip}) and 13 crystal field parameters (N_{cfp}) to vary gives a σ_{tot} of only 12.4 cm^{-1}. For comparison with other calculations in the literature which allow the barycenters of all the multiplets to vary, σ_{cf} is calculated here to be 10.8 cm^{-1}. This is slightly larger than our calculation when using the parameter values presented in Ref. 56, where only those low multiplet terms up to $^4G_{9/2}$ were included in the optimization (we could not reproduce the results in Ref. 56, probably due to some minor differences in free ion operators). As expected, the value of σ_{cf} was significantly reduced when only those low multiplets were included in our fitting. The residual error due to the difference between calculated and measured barycenters of multiplets can be gauged by the value σ_{fi}=24.0 cm^{-1}, which is much larger than σ_{cf}.

C. Theoretical results for YAP:Nd^{3+}

The experimental energy levels have been given by up to $^2P_{1/2}$ by Weber and Varitimos[35] and additional energy levels are available in Refs. 13, 37, and 40. As mentioned above, the energy level at 16 849 cm^{-1} assigned in Ref. 35 corresponds to an absorption hot hand. Our emission spectra have been assigned to the lowest energy level of $^2G(2)_{9/2}$ located at 46 718 cm^{-1}.

The only differences between our calculation and the one presented by Rukmini *et al.*[45] are that three more energy levels are included in the fitting and a few missed lines in the $\hat{m}_j$ (j=0,2,4) and $\hat{p}_k$ (k=2,4,6) operators are included in the program. These changes have only very minor effects upon the parameter values so we started with the parameter values presented previously[15] and followed the same procedure as in YAP:Er^{3+}. It is interesting that in the process of calculation the imaginary part of parameter B_4^6 was not well defined in Nd^{3+}, similar to the case of Er^{3+}. We also set it to be zero without affecting the residual error. It is well known that in general the set of parameter values correspond to a local minimum rather than to the global minimum of the residual error. Thus, after obtaining a local minimum we allowed some of those parameters with big uncertainties or small absolute values to change sign to test the stability of the parameter values. A few sets of similar parameter values were obtained with almost identical residual errors. The set of parameter values compatible with that obtained when starting with the Deb[43] crystal field parameters for YAP:Er^{3+} are presented in Table III.

The fitting of 100 levels by varying 15 free ion parameters (N_{fip}) and 13 crystal field parameters (N_{cfp}) gives a σ_{tot} of 15.5 cm^{-1}, which is larger than that for Er^{3+}. Contributions to this σ_{tot} are due to σ_{cf}=15.6 cm^{-1} and σ_{fi}=13.5 cm^{-1}. Compared to the Er^{3+} fitting, the much smaller σ_{fi} for Nd^{3+} means that the barycenters of multiplets are much better described by the resulting free ion parameters. This is also reflected in the much smaller uncertainty in the relevant free ion parameters for Nd^{3+} presented in Table III. The residual error due to crystal field splitting presented here is similar to that in the calculation without using correlation crystal field parameters presented by Rukmini *et al.*[45] It is well known that the residual errors can be further reduce by including correlation crystal-field interactions,[45] but their selection is rather arbitrary and is not attempted in this work.

V. CONCLUSIONS

The VUV excited emission and excitation spectra have been investigated for the systems YAP:Nd^{3+} and YAP:Er^{3+}. In each case, ultraviolet luminescence is observed from an f-electron multiplet term that is well-separated from its next-lowest neighbor: from $^2P_{3/2}$ (3384 cm^{-1} above $^2K_{15/2}+{}^4G_{7/2}$) for Er^{3+}, and from $^2G(2)_{9/2}$ [at 7198 cm^{-1} above $^2F(2)_{7/2}$] for Nd^{3+}. The transitions are electric dipole allowed at the C_s site symmetry of YAP so that the spectra comprise zero phonon lines almost exclusively at the spectral sensitivity employed. Nonradiative population of lower luminescent levels occurs to a greater extent for Er^{3+}. The f-d excitation spectra are partially masked by the YAP host absorption in each case. The d-f luminescence is not observed in both systems, due to nonradiative depopulation of the lowest d-electron level to energetically nearby f-electron levels in each case. These behaviors contrast with some other systems doped with Er^{3+} and Nd^{3+}.

In YAG:Nd^{3+}, fast d-f emission is observed, as well as f-f emission from $^2F(2)_{5/2}$ and $^4F_{3/2}$.[57] On comparing the intraconfigurational luminescence observed in these systems under VUV excitation, it is observed that the luminescent $^2F(2)_{5/2}$ level in YAG:Nd^{3+} is at ~8940 cm^{-1} lower energy than the luminescent $^2G(2)_{9/2}$ level in YAP:Nd^{3+}. This occurs because the lowest d-electron level is located at lower energy in YAG:Nd^{3+} than in YAP:Nd^{3+}. Therefore, the d-f emission is favored because of a sufficiently large energy gap as well as stepwise nonradiative population down to the $^2F(2)_{5/2}$ multiplet term. Thus the d-f emission intensity depends critically upon the energy gap below the lowest d-electron level. Furthermore, the interconfigurational Nd^{3+} emission was not observed in the hexachloroelpasolite host Cs_2NaYCl_6,[58] where the $4f^3 \rightarrow 4f^2 5d$ absorption bands commence at ~47 000 cm^{-1}, but *is* observed in Cs_2NaYF_6 where the corresponding bands are at sufficiently higher energy to provide a gap with $^2G(2)_{7/2}$.[59]

The VUV spectra of Er^{3+} have been studied in a variety of hosts (for example, Refs. 51 and 60–64) and both spin-

forbidden and spin-allowed *d-f* transitions are possible. However, as shown by the example of Table IV, the $4f^{11}$ configuration is expansive and *d-f* luminescence will only occur if the lowest *d*-electron level fortuitously falls in a gap between the *f*-electron levels. Thus, no *d-f* emission is observed for Er^{3+} in YPO_4,[61] but the appropriate energetic location of *d*-electron levels within the ~5000–7000 cm^{-1} gap between $^2F(2)_{5/2}$ and $^2D(2)_{3/2}$ permits interconfigurational transitions from both high-spin and low-spin *d* states to occur for Er^{3+}, for example in $LiYF_4$.[62–64] The *d*-electron levels are too low in energy in our present case of YAP:Er^{3+} so that nonradiative relaxation to *f*-electron levels becomes dominating.

Energy level calculations have been presented for Er^{3+} and Nd^{3+} doped into YAP. One hundred crystal field levels were fitted in each case and the standard deviation σ_{tot} was 14 ± 2 cm^{-1}. Since the derived energy levels from the analysis of the Nd^{3+} $^2G(2)_{9/2}$ luminescence spectra are not sufficiently accurately determined, these values have been listed for comparison with calculation. Satisfactory agreement is observed in most cases, except for the $^2L_{17/2}$ levels. However, there is no evidence to suggest that emission occurs from another multiplet term, except for $^4F_{3/2}$. A detailed comparison of the derived energy parameters with those from other members of the Ln^{3+} series in YAP will be presented elsewhere.

The scalar crystal-field strength parameter defined in the work of Auzel[65] can be expressed as

$$N_v = \sum_{k=2,4,6} \frac{4\pi}{2k+1} \sum_{q=-k}^{k} |B_{|q|}^k|^2. \quad (9)$$

The calculated values are 3406 cm^{-1} for Nd^{3+} and 2159 cm^{-1} for Er^{3+}, which follow the general trend that the crystal-field strength decreases as the number of electrons in the *f* shell increases due to the contraction of *f* orbitals.

ACKNOWLEDGMENTS

We acknowledge financial support for this study under the Hong Kong University Grants Council Research Grant No. CityU 102304. C.K.D. acknowledges the support under the City University Research Grant No. 9360123. This work was also supported by RFBR Grants Nos. 05-02-1730 and 06-02-39027-NNSF and the Estonian Science Foundation (Grant No. 6538).

[1] R. Diehl and G. Brandt, Mater. Res. Bull. **10**, 85 (1975).
[2] L. Vasylechko, A. Matkovskii, D. Savytskii, A. Suchocki, and F. Wallrafen, J. Alloys Compd. **291**, 57 (1999).
[3] T. Tomiki, M. Kaminao, Y. Tanahara, T. Futemma, M. Fujisawa, and F. Fukudome, J. Phys. Soc. Jpn. **60**, 1799 (1991).
[4] T. Tomiki, Y. Ganaha, T. Shikenbaru, T. Futemma, M. Yuri, Y. Aiura, H. Fukutani, H. Kato, T. Miyahara, A. Yonesu, and J. Tamashiro, J. Phys. Soc. Jpn. **63**, 1976 (1994).
[5] T. Tomiki, F. Fukudome, and M. Kaminao, J. Lumin. **40-41**, 379 (1988).
[6] C. Lushchik, E. Feldbach, A. Frorip, M. Kirm, A. Lushchik, A. Maaroos, and I. Martinson, J. Phys.: Condens. Matter **6**, 11 177 (1994).
[7] D. M. Bercha, K. Z. Rushchanskii, M. Sznajder, A. Matkovskii, and P. Potera, Phys. Rev. B **66**, 195203 (2002).
[8] H. C. Gupta and P. Ashdhir, J. Solid State Chem. **146**, 287 (1999).
[9] P. Alain and B. Piriou, Phys. Status Solidi B **43**, 669 (1971).
[10] V. A. Antonov, P. A. Arsenev, K. E. Bienert, and A. V. Potemkin, Phys. Status Solidi A **19**, 289 (1973).
[11] V. L. Donlan and A. A. Santiago, J. Chem. Phys. **57**, 4717 (1972).
[12] A. A. Kaminskii, *Laser Crystals* (Springer-Verlag, Berlin, 1981). Chap. 4.
[13] C. A. Morrison and R. P. Leavitt, *Handbook on the Physics and Chemistry of Rare Earths*, edited by K. A. Gschneidner, Jr. and L. Eyring (North Holland, Amsterdam, 1982), Chap. 46.
[14] A. A. Kaminskii, V. S. Mironov, A. Kornienko, S. N. Bagaev, G. Boulon, A. Brenier, and B. D. Bartolo, Phys. Status Solidi A **151**, 231 (1995).
[15] M. Pollnau, E. Heumann, and G. Huber, J. Lumin. **60**&61, 842 (1994).
[16] M. J. Weber, M. Bass, T. E. Varitimos, and D. P. Bua, IEEE J. Quantum Electron. **9**, 1079 (1973).
[17] M. J. Weber, M. Bass, and G. A. DeMars, J. Appl. Phys. **42**, 301 (1971).
[18] I. V. Mochalov, Phys. Status Solidi A **55**, 79 (1979).
[19] N. Pelletier-Allard and R. Pelletier, J. Alloys Compd. **275-277**, 374 (1998).
[20] J. Frauchiger, W. Lüthy, P. Albers, and H. P. Weber, Opt. Lett. **13**, 964 (1988).
[21] M. Stalder, W. Lüthy, and H. P. Weber, Opt. Lett. **12**, 602 (1987).
[22] J. Breguet, A. F. Umyskov, S. G. Semenkov, W. Lüthy, H. P. Weber, and I. A. Shcherbakov, IEEE J. Quantum Electron. **28**, 2563 (1992).
[23] H. Xu, L. Zhou, Z. Dai, and Z. Jiang, Physica B **324**, 43 (2002).
[24] S. Georgescu, V. Lupei, M. Trifan, R. J. Sherlock, and T. J. Glynn, J. Appl. Phys. **80**, 6610 (1996).
[25] V. P. Danilov, A. M. Prokhorov, M. I. Studenikin, D. Schmid, L. O. Schwan, and R. Glasmacher, Phys. Status Solidi A **176**, 593 (1999).
[26] M. Chua, S. Xia, and P. A. Tanner, J. Phys.: Condens. Matter **15**, 7423 (2003).
[27] J. Wang and D. J. Simkin, Phys. Rev. B **52**, 3309 (1995).
[28] A. Brenier and A. M. Jurdyc, J. Lumin. **69**, 131 (1996).
[29] R. Scheps, IEEE J. Quantum Electron. **31**, 309 (1995).
[30] D. J. Simkin, J. A. Koningstein, P. Myslinski, S. A. Boothroyd, and J. Chrostowski, J. Appl. Phys. **73**, 8046 (1993).
[31] R. Scheps, IEEE J. Quantum Electron. **30**, 2914 (1994).
[32] A. J. Silversmith, W. Lenth, and R. M. Macfarlane, Appl. Phys. Lett. **51**, 1977 (1987).
[33] R. Francini, S. Pietrantoni, M. Zambelli, A. Speghini, and M. Bettinelli, J. Alloys Compd. **380**, 34 (2004).
[34] H. Yang, Z. Dai, and Z. Sun, J. Lumin. **124**, 207 (2007).

[35] M. J. Weber and T. E. Varitimos, J. Appl. Phys. **42**, 4996 (1971).
[36] N. Pelletier-Allard, R. Pelletier, C. Tiseanu, and V. Lupei, J. Lumin. **62**, 61 (1994).
[37] T. T. Basiev, A. Yu Bergachev, and Yu V. Orlovskii, Tr. Inst. Fiziol., Akad. Nauk. Graz. SSR **46**, 3 (1994).
[38] A. V. Rasuleva and V. I. Solomonov, Phys. Solid State **47**, 1489 (2005).
[39] O. L. Antipov, O. N. Eremeikin, and A. P. Savikin, Quantum Electron. **32**, 793 (2002).
[40] M. A. Dubinskii and A. L. Stolov, Sov. Phys. Solid State **27**, 1315 (1985).
[41] J. J. Romero, E. Montoya, L. E. Bausa, F. Agullo-Rueda, M. R. B. Andreeta, and A. C. Hernandes, Opt. Mater. **24**, 643 (2004).
[42] N. Karayianis, D. E. Wortman, and C. A. Morrison, Solid State Commun. **18**, 1299 (1976).
[43] K. K. Deb, J. Phys. Chem. Solids **43**, 819 (1982).
[44] E. Rukmini, A. Renuka Devi, and C. K. Jayasankar, Physica B **193**, 166 (1994).
[45] E. Rukmini, C. K. Jayasankar, and M. F. Reid, J. Phys.: Condens. Matter **6**, 5919 (1994).
[46] G. Zimmerer, Nucl. Instrum. Methods Phys. Res. A **308**, 178 (1991).
[47] M. J. Weber, Phys. Rev. B **8**, 54 (1973).
[48] M. J. Weber, T. E Varitimos, and B. H. Matsinger, Phys. Rev. B **8**, 47 (1973).
[49] A. J. Wojtowicz, Nucl. Instrum. Methods Phys. Res. A **486**, 201 (2002).
[50] P. Dorenbos, J. Lumin. **91**, 91 (2000).
[51] L. van Pieterson, M. F. Reid, R. T. Wegh, S. Soverna, and A. Meijerink, Phys. Rev. B **65**, 045113 (2002).
[52] L. van Pieterson, M. F. Reid, G. W. Burdick, and A. Meijerink, Phys. Rev. B **65**, 045114 (2002).
[53] S. Kammoun and M. Kamoun, Phys. Status Solidi B **229**, 1321 (2002).
[54] N. M. Khaidukov, M. Kirm, S. K. Lam, D. Lo, V. N. Makhov, and G. Zimmerer, Opt. Commun. **184**, 183 (2000).
[55] W. T. Carnall, G. L. Goodman, K. Rajnak, and R. S. Rana, J. Chem. Phys. **90**, 3443 (1989).
[56] J. M. O'Hare and V. L. Donlan, Phys. Rev. B **15**, 10 (1977).
[57] L. Ning, P. A. Tanner, V. V. Harutunyan, E. Aleksanyan, V. N. Makhov, and M. Kirm, J. Lumin. (to be published).
[58] A. Collombet, Y. Guyot, C. S. K. Mak, P. A. Tanner, and M.-F. Joubert, J. Lumin. **94**, 39 (2001).
[59] P. A. Tanner, L. Ning, V. N. Makhov, N. M. Khaidukov, and M. Kirm, J. Phys. Chem. B **110**, 12113 (2006).
[60] N. M. Khaidukov, S. K. Lam, D. Lo, V. N. Makhov, and N. V. Suetin, Opt. Mater. **19**, 365 (2002).
[61] W. Jia, Y. Zhou, D. A. Keszler, J.-Y. Jeong, K. W. Jang, and R. S. Meltzer, Prog. Solid State Chem. **2**, 48 (2005).
[62] M. Kirm, V. N. Makhov, M. True, S. Vielhauer, and G. Zimmerer, Phys. Solid State **47**, 1416 (2005).
[63] R. T. Wegh, H. Donker, and A. Meijerink, Phys. Rev. B **57**, R2025 (1998).
[64] R. T. Wegh and A. Meijerink, Phys. Rev. B **60**, 10820 (1999).
[65] F. Auzel, Opt. Mater. **19**, 89 (2002).